International Journal of Civil Engineering

Water-Hydraulic Structure

Dynamic pressure analysis at chute flip buckets of five dam model studies

O. Nazari[1], E. Jabbari[2]*, H. Sarkardeh[3]

Received: February 2013, Revised: June 2013, Accepted: July 2013

Abstract

To dissipate energy and invert excessive discharge flow away from high dams into plunge pool, flip buckets are commonly designed and optimized by hydraulic model studies. In the present study, performance of chute flip buckets in different hydraulic and geometry conditions was investigated using experimental data of five different physical models. The collected experimental data such as Froude number, radius of flip bucket and slope of chute covered a wide range of chute flip buckets in prototype. By analyzing the data, relations for dynamic values of maximum and minimum pressures and their location along the flip bucket were extracted. Moreover, pressure distribution along the central axis of flip bucket was defined. Finally, results of the present research were compared with that of the other researches. Results of this study could be used in the design of chute flip buckets in hydraulic engineering.

Keywords: *Dams, Physical model, Flip bucket, Pressure distribution, Dynamic pressure.*

1. Introduction

Energy dissipation downstream of large dams is a serious and problematic subject. Using flip bucket is recommended when flow velocity is larger than about 15–20 m/s [1, 2]. Flip buckets are widely used because they allow the control of large quantities of excess hydraulic energy in a technically sound and a hydraulically safe way [3, 4]. A great deal of investigation on the flow characteristics of ski jumps have been introduced in the literature. Pressures over buckets have been computed and observed by Balloffet [5]. Henderson and Tierney demonstrated that for small ratio of hydraulic head and radius of bucket, the two dimensional (2D) computations and observations match if only the deflection angle is at least 45^{o} [6].

Chen and Yu figured the pressure distribution over a cylindrical bucket by using the potential flow equations for different deflection angles [7]. Lenau and Cassidy demonstrated that the effect of viscosity in bucket flow is insignificant [8]. Varshney and Baja j [9], Rajan and Rao [10] and Rao [11] also carried out investigations on major parameters of ski jump design at dams.

Juon and Hager investigated the flip bucket hydraulics without and with deflectors in a laboratory model study related to the circular shaped bucket geometry [12].

In addition, Heller et al. performed investigation on the ski jump hydraulics in a laboratory model study related to the circular shaped bucket geometry [13].

Steiner et al. also investigated the ski jump hydraulics in a laboratory model study related to the circular shaped bucket geometry for ease in construction and based on three dimensional (3D) flip bucket designs [14]. In the most recent work, Yamini and Kavianpour presented dynamic pressure distribution over the simple circular flip bucket [15]. Kermannejad et al. also investigated the dynamic pressures due to the impact of a ski jump out of a flip bucket downstream of a chute spillway model. Their results showed that the pressure coefficient is highly sensitive to horizontal and vertical distances from the impact location as well as to the impact angle [16]. In parallel with the experimental works, some numerical studies also were performed by different researchers [17,18,19,20,21].

Although ski jumps have been introduced as energy dissipation systems and many flip buckets for this purpose with various geometries are in operation, there has been few design consideration over chute flip buckets. In the present study, circular arc buckets with no curvature in plan and the steeply sloping chute approach channel were investigated. By using five different physical model data, experimental equations were extracted for values of maximum and minimum fluctuation pressures and their location along the flip bucket bottom. Moreover, pressure distribution along the central axis of flip bucket was presented. Finally results of the present research were compared with the other researches data.

** Corresponding author: jabbari@iust.ac.ir*

1 M.Sc. Student, School of Civil Engineering, Iran University of Science and Technology, Narmak, P.O. Box 16765-163, Tehran, Iran

2 Associate Professor, School of Civil Engineering, Iran University of Science and Technology, Narmak, P.O. Box 16765-163, Tehran, Iran

3 Assistant Professor, Department of Civil Engineering, Faculty of Engineering, Hakim Sabzevari University, Sabzevar, Iran

[DOI: 10.22068/IJCE.13.1.45]

2. Physical Models and Experimental Tests

To achieve a comprehensive study on flip buckets, five different physical models were selected. To make using different data possible, all the parameters were described and detailed first as shown in schematic view of a flip bucket spillway in Figure 1.

where W= Bucket width, R= Bucket radius, θ= Takeoff angle, β= deflection angle, α= $\tan^{-1}$ (1:Z) chute slope, $L_t = R(\sin\alpha + \sin\theta)$ Total bucket length, V_0= velocity of entrance flow, h_0 = height of entrance flow, T_b = Thickness of takeoff lip x_1 = Rsinα, x_2 = Rsinθ and h_s = Height of bucket from the bed. Experiments were carried out in different flow conditions and different bucket geometries (Figure 2). A summary of used data in the prototype scale is also presented in Table 1.

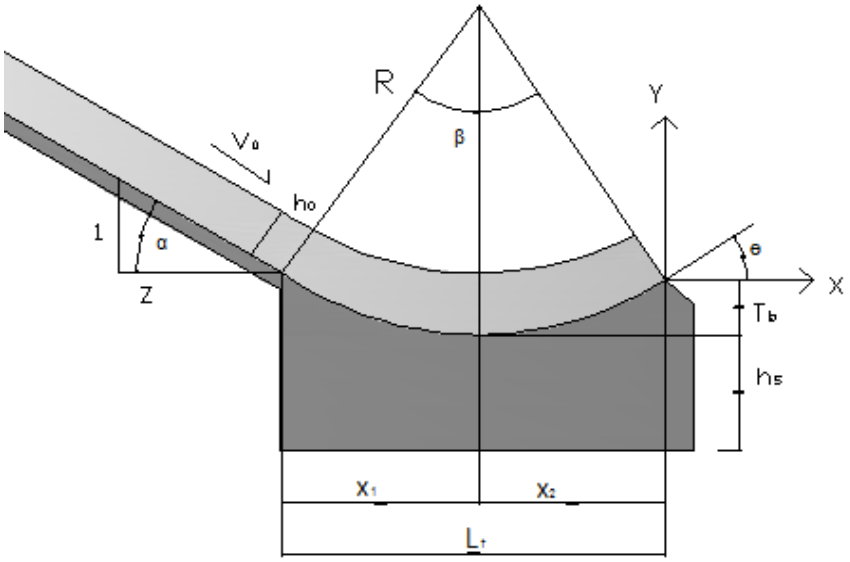

Fig. 1 Schematic view of flip bucket details

Flip Bucket Model of Jareh Dam

Flip Bucket Model of Azad Dam

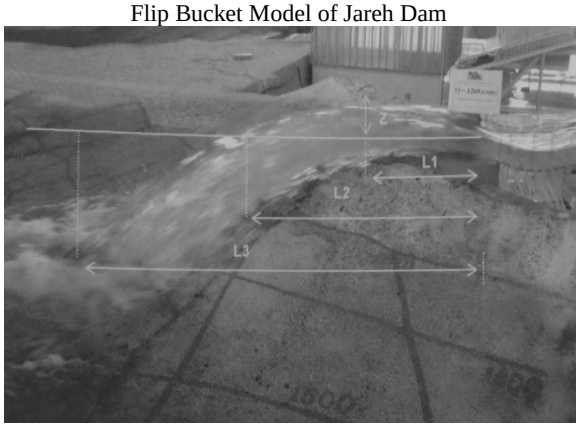

Flip Bucket Model of Ajab Shir Dam

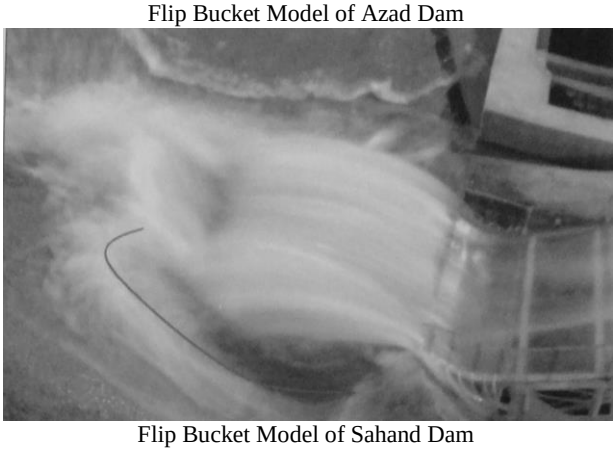

Flip Bucket Model of Sahand Dam

[DOI: 10.22068/IJCE.13.1.45]

Flip Bucket Model of Kamal Saleh Dam

Fig. 2 Used physical models in this study

Table 1 Hydraulic model parameters used in the present study (in prototype)

Dam	scale	Q (m^3/s)	h_0 (m)	v_0 (m/s)	Fr_0	W (m)	R (m)	L_t (m)	α^o	β^o	θ^o
Jareh	1:50	500	1.400	26.97	7.28	25	25	19.08	13.50	45.50	32.00
		1000	1.798	29.35	6.99						
		1500	2.383	32.70	6.76						
		1900	2.867	32.44	6.12						
		2100	3.150	33.68	6.06						
		2850	4.067	35.33	5.59						
Azad	1:33	500	0.990	28.64	9.19	30	15	11.73	20.00	46.14	26.14
		800	1.610	32.71	8.23						
		1226	2.003	34.59	7.80						
		1545	2.387	36.97	7.64						
		2290	3.110	38.01	6.88						
Ajab Shir	1:28	800	2.333	27.66	5.78	16	18	10.89	10.53	35.53	25.00
		1200	3.160	27.78	4.99						
		1300	3.427	28.11	4.85						
Sahand	1:40	800	0.933	22.23	7.35	35	13	13.80	23.50	64.71	41.21
		1510	1.567	23.6	6.02						
		1850	1.833	24.6	5.80						
Kamal Saleh	1:40	606	1.013	28.84	9.15	30	15	11.71	16.33	46.33	30.00
		941	1.600	30.56	7.71						
		2260	2.787	31.73	6.07						
		606	1.013	28.84	9.15		18	11.64	16.33	37.79	21.46
		941	1.600	30.56	7.71						
		2260	2.787	31.73	6.07						

Physical models of flip buckets in the present work were constructed based on Froude similarity between model and prototype. Selected scales were concluded from proposed scale effect criteria by other researchers. For example if Reynolds Number ($Re = VR_h/\nu$) be more than 10^5, the viscosity effect in the model is negligible and if depth of water be more than 20mm, the effect of surface tension is negligible [22, 23]. In the all experiments of this study, Re was more than 2×10^7 and depth of flow was more than 26mm. Experimental models of chute buckets were built with Plexiglas to make visualization of flow possible. In the all experiments, by installing pressure transducers with 0.1% accuracy on the bottom of flip buckets, dynamic pressure fluctuations were recorded. Figure 3 shows the location of installed pressure transducers. The rate of pressure sampling in all experiments was 100HZ.

[DOI: 10.22068/IJCE.13.1.45]

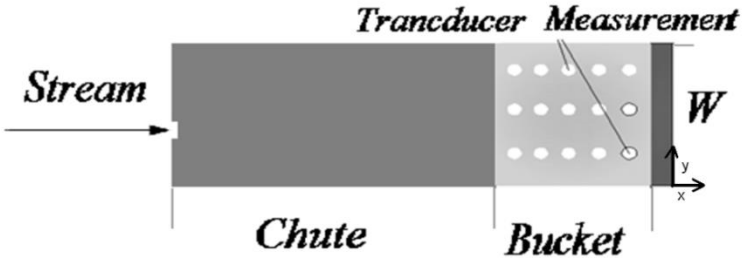

Fig. 3 Plan view of pressure transducer locations over flip bucket bottoms

3. Dimensional Analysis

To conclude relations among physical quantities in physical models, dimensional analysis is required. In the present research, the dependent variable P could be expressed in terms of other variables by the following function:

$$P = f(h_0, V_0, g, \mu, \sigma, \alpha, \beta, \theta, R, \rho) \quad (1)$$

where p is pressure, g is the acceleration due to gravity, μ is viscosity, σ is the surface tension, ρ is density and the other parameters described in previous section. Using Buckingham π-theorem dimensionless parameters are as bellow:

$$\frac{P}{\rho V_0^2} = f(\tan\alpha, \tan\beta, \tan\theta, \frac{gh_0}{V_0^2}, \frac{R}{h_0}, \frac{\mu}{\rho h_0 V_0}, \frac{\sigma}{\rho h_0 V_0^2}) \quad (2)$$

Since the flow is fully turbulent, viscosity and surface tension have a negligible effect on bucket flow conditions [22,23], hence, the above equation can be simplified as:

$$\frac{p}{\rho V_0^2} = a_0 (\frac{R}{h_0})^{a_1} (\frac{1}{Fr_0^2})^{a_2} (\tan\alpha)^{a_3} (\tan\beta)^{a_4} (\tan\theta)^{a_5} \quad (3)$$

where Fr_0 ($=V_0/\sqrt{gh_0}$) is the entrance Froude Number and R/h_0 is relative curvature of bucket. The power model is widely used in engineering as the structure of the derived empirical models. Coefficients are fitted using a logarithmic transformation of data. Equations can be fitted using ordinary least squares [24].

$$\ln(\frac{P}{\rho V_0^2}) = \ln a_0 + a_1 \ln(\frac{R}{h_0}) + a_2 \ln(\frac{1}{Fr_0^2}) + a_3 \ln(\tan\alpha) + a_4 \ln(\tan\beta) + a_5 \ln(\tan\theta) \quad (1)$$

4. Experimental Results

Results of the present experimental study and derived equations consist of maximum and minimum dynamic pressures, location of their occurrence and dynamic pressure distribution along the bucket are presented in this section. Finally the derived equations are compared with other experimental data.

4.1. Value of maximum dynamic pressure

When flow passes the bucket, pressures fluctuate irregularly over the bucket. Maximum, minimum and average are the values of the pressure desired to be determined for the design purposes (Figure 4).

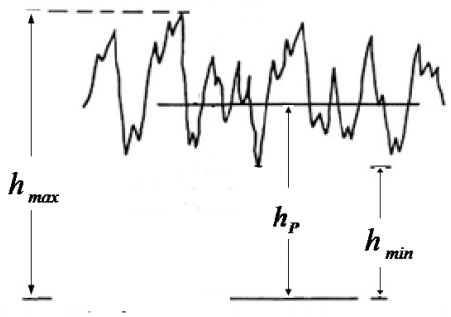

Fig. 4 Pressure fluctuation head characteristics

In Figure 4, h_{max} (P_{max}/γ) is the maximum head, h_{min} (P_{min}/γ) is the minimum head and h_p (P_p/γ) is the average head of the dynamic pressure fluctuations. By using linear regression and elimination of *tanθ* and *tanβ*, due to their inconsiderable effects on the pressure fluctuations; the best fitted relation is obtained as:

$$\frac{p_{\max}}{\rho V_0^2} = 1.016 (\frac{1}{Fr_0^2})^{0.2} (\tan\alpha)^{-0.264} (\frac{R}{h_0})^{-0.76} \quad (5)$$

where P_{max} is the maximum pressure fluctuation (Figure 4). The collected data from experiments and the results of the extracted relation are compared in Figure 5.

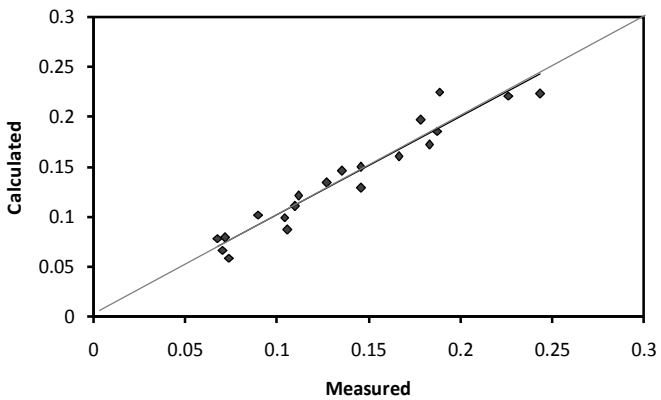

Fig. 5 Measured and calculated data for P_{max} (Equation 5)

[DOI: 10.22068/IJCE.13.1.45]

As can be seen from Figure 5, there is good agreement between the measured and calculated data (correlation factor = r^2 = 0.90).

4.2. Value of minimum dynamic pressure

Cavitation is one of the important and destructive hydraulic phenomena which occur in high velocity and low pressure conditions. Sometimes over hydraulic structures, by increasing velocity and existing small roughness at flow walls, pressure decreases. Decreasing local pressure may cause vapor pressure and creation of bubbles. Produced bubbles, distribute in the flow and transport farther to a place with high pressure. In this time, they will explode and produce noise and huge impact stresses on the walls. In the present study, value of minimum dynamic pressure is derived according to the experimental data as the following equation to predict possibility of cavitation:

$$\frac{p_{\min}}{\rho V_0^2} = 1.53\left(\frac{1}{Fr_0^2}\right)^{0.61}(\tan\alpha)^{-0.602}\left(\frac{R}{h_0}\right)^{-0.734} \quad (6)$$

By plotting measured data against calculated data from the above relation, it can be seen that the obtained relation predicts the minimum dynamic pressure over the flip bucket appropriately (Figure 6). The correlation factor r^2 is about 0.87.

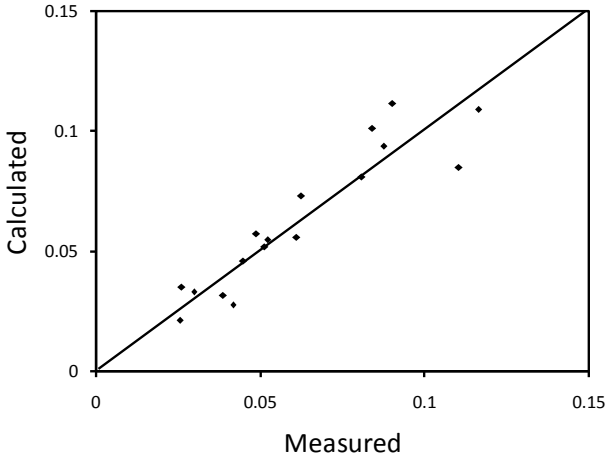

Fig. 6 Calculated and measured data for P_{min} (Equation 6)

4.3. Location of minimum dynamic pressure

Regarding experimental data and defining the entrance number as $\zeta = Fr_0^{0.65} \times tan\alpha$ and dimensionless location of the minimum dynamic pressure as $X_{Pmin} = x_{Pmin}/L_t$ (x_{Pmin} is the location of the minimum dynamic pressure from bucket lip), in $X_{Pmin} \approx 0.1$ and $X_{Pmin} \approx 0.9$, minimum dynamic pressure can occur in the entrance and the terminal sections of flip bucket (Figure 7).

In Figure 7, two parts could be highlighted in the view of the occurrence of cavitation. If $\zeta < 0.9$ then $X_{Pmin} \approx 0.1$ and if $\zeta > 0.9$ then $X_{Pmin} \approx 0.9$.

Cavitation index is also defined as $\delta = (h - h_v)/(V^2/2g)$ in which h is the absolute pressure head and h_v is the vapor pressure head. In order to observe the values of the cavitation index at the bottom of the flip bucket, cavitation indices were calculated and plotted for various ranges of Fr (Figure 8).

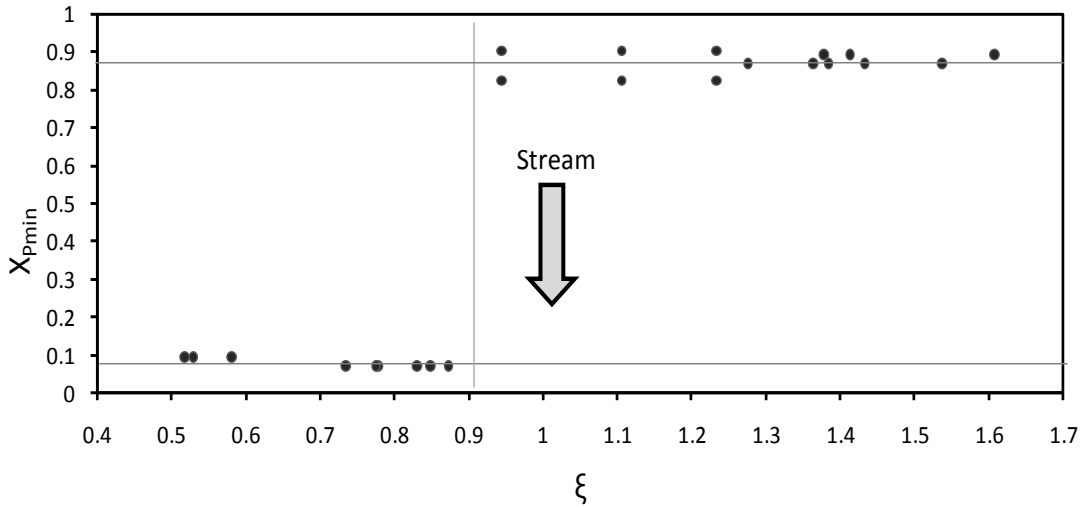

Fig. 7 Dimensionless location of the X_{Pmin} against entrance number ζ

[DOI: 10.22068/IJCE.13.1.45]

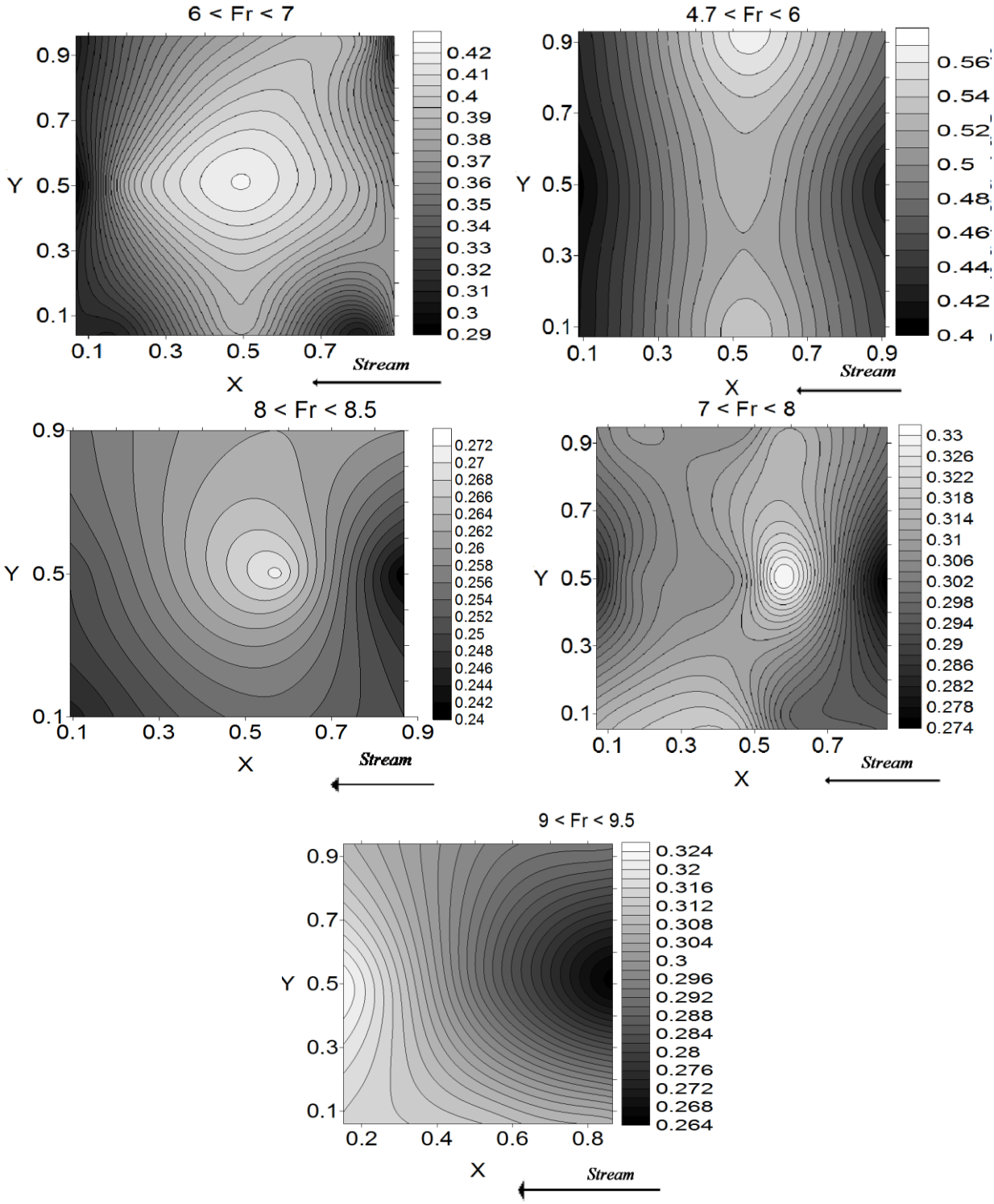

Fig. 8 Cavitation index contours along the bucket

As it could be seen in Figure 8, the entrance and exit sections of the bucket encounter cavitation hazard. In lower Fr_0, at the entrance and exit sections, cavitation index is lower than the other points. By increasing Fr_0, probability of cavitation is limited to the entrance section.

4.4. Dynamic pressure distribution along the bucket

Pressure distribution along a flip bucket could help to understand the dynamic pressures head h_p in different conditions. Figure 9 shows the characteristics of the dynamic pressure distribution.

In Figure 9, h_{PM} is the maximum dynamic pressure head over the bucket and x_{PM} represents the location of the maximum dynamic pressure over the bucket. h_{PM} could be obtained as follows:

$$\frac{h_{PM}}{V_0^2/g} = 1.034\left(\frac{1}{Fr_0^2}\right)^{0.319}(\tan\alpha)^{-0.218}\left(\frac{R}{h_0}\right)^{-0.765} \quad (7)$$

[DOI: 10.22068/IJCE.13.1.45]

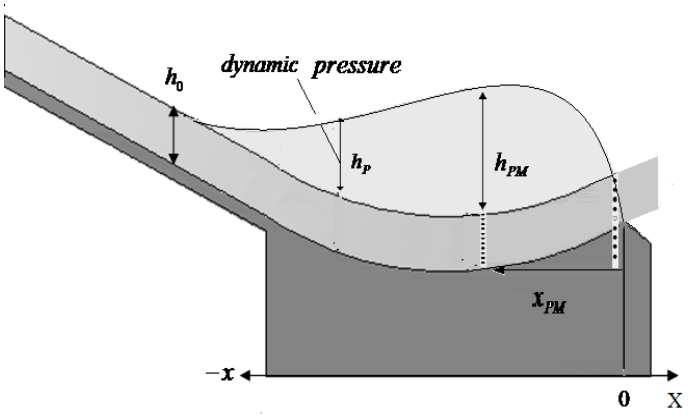

Fig. 9 Schematic view of the dynamic pressure head characteristics

By using the collected data from experiments and results of extracted formula and plotting them, r^2 is about 0.92 (Figure 10).

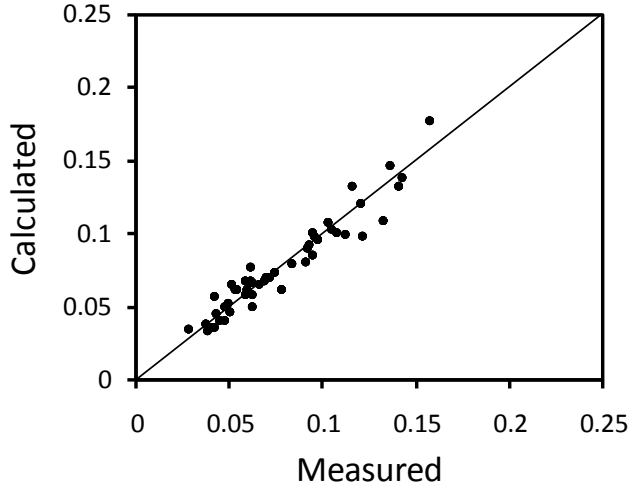

Fig. 10 Comparison between measured and calculated data from Equation 7

x_{PM} (location of maximum measured dynamic pressure head) in flip bucket bottom is also an important factor in hydraulic design. To make the presentation of the location of the maximum dynamic pressure head occurrence easy, length of the flip bucket (L_t) is divided into two different parts, $x_1 = R\sin\alpha$ and $x_2 = R\sin\theta$ (Figure 11). In Figure 12, x_{pM}/L_t is plotted versus Fr.

As can be seen from Figure 12, x_{pM} is in range of $(0.45 - 0.6)L_t$, This means the effect of Fr is negligible and therefore equation for calculating x_{pM} is based on the chute angle and take off angle. Figure 13 shows collected experimental data in different conditions (x_{PM}/x_2 *versus* $\eta = \sin\theta/(\sin\alpha+\sin\theta)$ = Angle number) and fitted Equation 8 with the correlation factor of $r^2 = 0.73$.

$$\frac{x_{PM}}{x_2} = 0.492\left(\frac{\sin\theta}{\sin\alpha+\sin\theta}\right)^{-1.12} \quad (8)$$

It should be noted that if $\sin\alpha = 0$ (horizontal approach channel), $x_{pM} \approx 0.5x_2$ (if $\sin\alpha = 0$ then $L_t = x_2$).

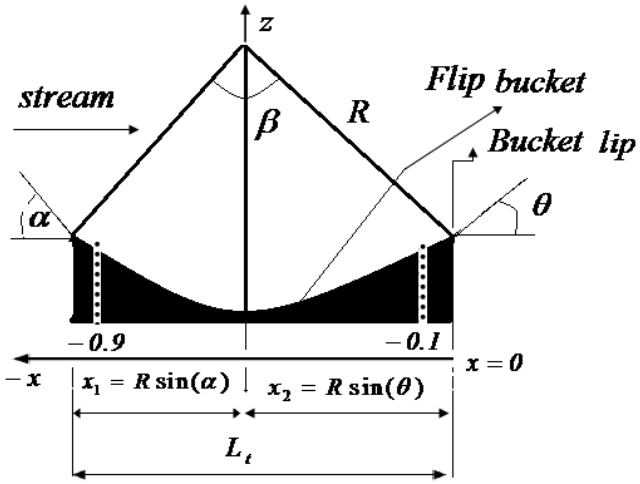

Fig. 11 Parts of flip bucket

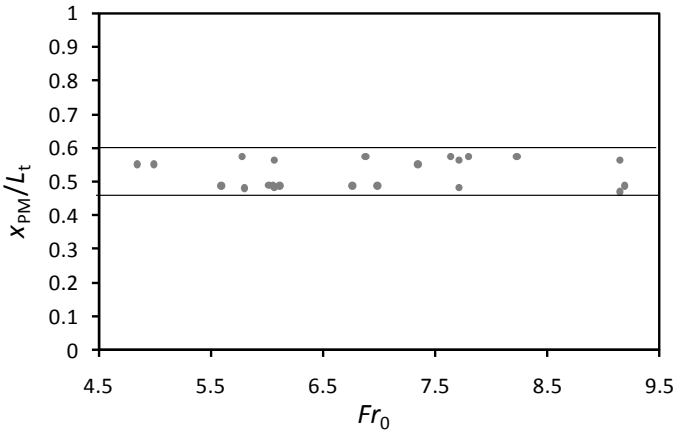

Fig. 12 x_{pM} along the bucket length

According to Figure 13 and Equation 8, x_{PM} is limited to the x_2 part of the flip bucket (Figure 11) only and in the range of $x_{PM} = (0.7 - 1.0)x_2$.

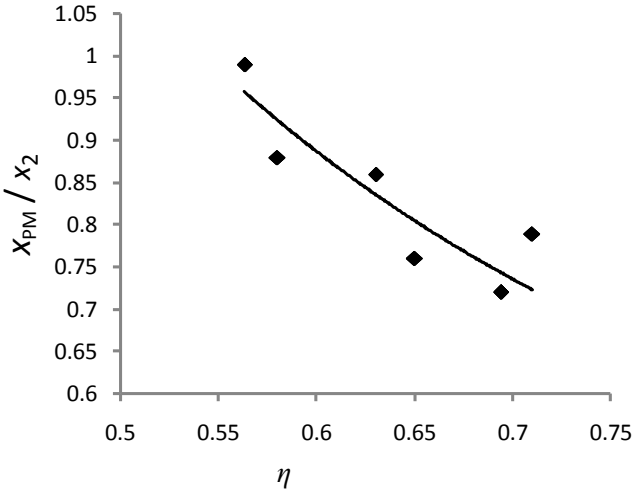

Fig.13 x_{PM} versus Angle number η

In order to determine the dynamic pressure distribution head along the flip bucket, a wide range of entrance flow conditions $4.7 \le Fr_0 \le 9.5$ was used. The relative pressure $P^* = h_P/h_{PM}$ was plotted along the normalized location

[DOI: 10.22068/IJCE.13.1.45]

factor $X_{pM} = x/x_{pM}$ where $x = 0$ is the takeoff point (Figure 14).

As can be seen from Figure 14, two different relations were derived for distribution of the dynamic pressure head as bellow:

$$P^* = (-X_{PM}^{0.65}) \exp(0.72+0.72X_{PM})^{0.8} \quad \text{for } -1 \leq X_{PM} \leq 0 \tag{9}$$

$$P^* = 0.98 \exp[(-0.75 X_{PM})^3 \times (1.4+X_{PM})]^{0.1} \quad \text{for } X_{PM} \leq -1 \tag{10}$$

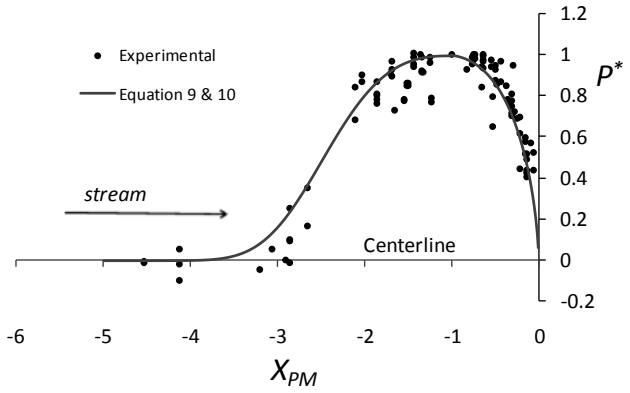

Fig. 14 Distribution of maximum pressure

4.5. Comparison between the results of this study and results of other researches

Results of the present research were compared with other similar researches. Equations 11 and 12 are proposed for dynamic pressure respectively as follows [12, 13]:

$$h_{pM}/h_0 = \tau B^2 \tag{12}$$

$$h_{pM}/h_0 = B^2 \quad \text{if} \quad [(h_0/R)(40^0/\beta)]<0.2 \tag{13}$$

where $B = (h_0/R)^{0.5} Fr_0$ and τ = fitting parameter ($\tau = 1$ for $B < 1.5$ and $\tau = 1.3B^{-0.5}$ for $B > 1.5$).

Hager et al. investigated the maximum dynamic pressure head h_{pM} based on the theoretical dynamic pressure head by a potential flow with concentric streamlines of radius R and also studied the dynamic pressure head distribution along the flip bucket and determined the relative pressure head $P^* = h_p/h_{pM}$ as a function of $X_{pM} = x/x_{pM}$ [13].

$$P^* = [X_{pM} \exp(1-X_{PM})]^{1.5} \tag{13}$$

Equation 7 of the present study was compared with the Equations 11 and 12 in Figure 15 [12, 13].

As can be seen from Figure 15, results of this study overestimate the maximum dynamic pressure over the flip bucket in comparison with the Equations 11 and 12 [12, 13]. The reason could be described by existing chute slope in the recent study which has a meaningful effect on increasing the maximum dynamic pressure head. Dynamic pressure head distribution also was compared with Equation 13 [13].

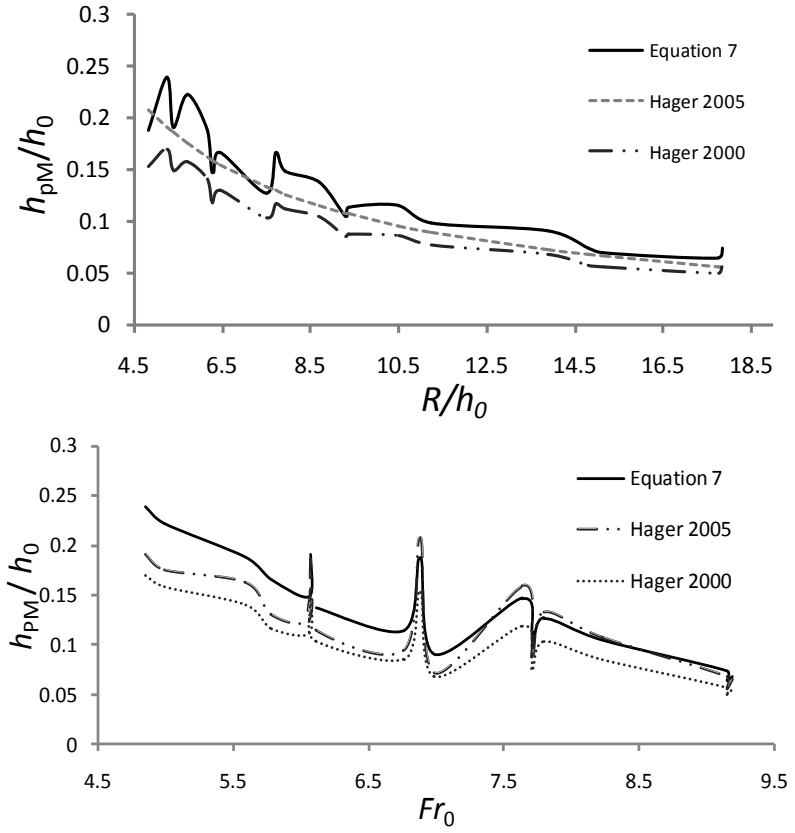

Fig. 15 Comparison between Equation 7 and Hager et al. (2000 and 2005)

[DOI: 10.22068/IJCE.13.1.45]

Fig. 16 shows that along the bucket, Equation 13 predicts pressures less than that of is presented in this research and at upstream channel the results are inverse [13]. The reason as mentioned before may be using a flat upstream channel by Hager et al. while a sloppy upstream channel has been used for the present study [13]. From Fig. 16 it could also be concluded that the maximum pressure is predicted the same in similar location by the both researches.

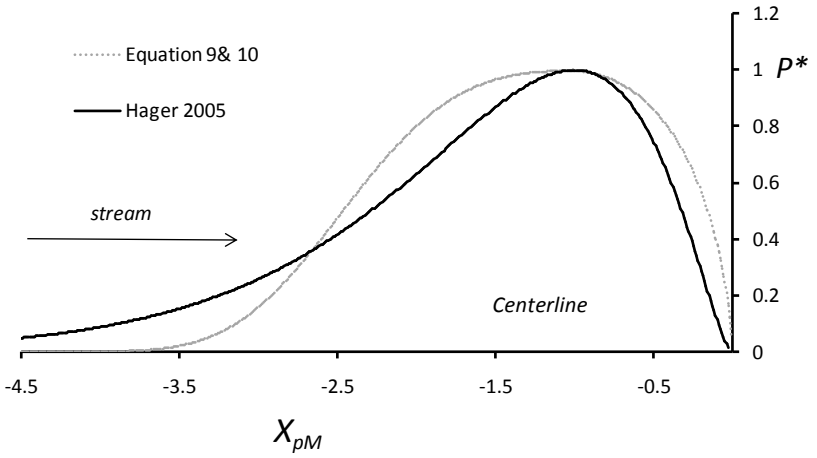

Fig. 16 Comparison between Hager et al. (2005) and Equations 9 and 10

5. Conclusions

Determining maximum and minimum of dynamic pressures and their locations are very important in the design of flip bucket structures. In this research, to have a comprehensive view about flip buckets, many experimental data from five flip bucket structures with a wide range of entrance flow conditions were used. The main parameters which were investigated in this involved relative bucket curvature (R/h_0), chute spillway slope ($tan\alpha$) bucket deflection angle (β), takeoff angle (θ) and approach Froude number (Fr_0). Relations were extracted for the maximum and minimum pressures fluctuations over the flip bucket with the Froude number, the relative radius of flip bucket and the chute slope as relevant dimensionless parameters. A relation was extracted for the maximum dynamic pressure and also location of the maximum and minimum values of dynamic pressure which depends on takeoff angle and chute slope, was determined. It is concluded that, x_{PM} was in the range of 0.45 to 0.6 of the length of flip bucket (L_t) and X_{Pmin} occurs in the entrance (≈ 0.9) and end (≈ 0.1) of the flip bucket. The dynamic pressure distribution along the bucket was figured based on the two proposed equations, one for $-1 \leq x_{PM} \leq 0$ and another for $x_{PM} \leq -1$. It was concluded that the slope of the upstream chute of the bucket has a meaningful effect on the dynamic pressures. Moreover, cavitation index along the flip bucket was calculated and presented for different hydraulic conditions. Finally, the concluded results were compared with other researches.

Acknowledgements: The Authors would like to thank from Water Research Institute (WRI), Tehran, Iran for their kindly cooperation in using physical model data.

Notations

W = filp bucket width;
R = flip bucket Radius;
θ = take off angle;
$\alpha = \tan^{-1}(1:Z)$ = Slop angle of chute;
β = deflection angle;
$L_t = R(sin\alpha+sin\theta)$ total bucket length;
V_0 = velocity of entrance flow;
h_0 = height of entrance flow;
T_b = thickness of take off ;
x_1 = upstream length of bucket;
x_2 = downstream length of bucket;
h_s = height of bucket from the bed;
Q = discharge flow;
P = pressure;
g = acceleration due to gravity;
μ = viscosity;
σ = surfer tension;
ρ = density;
$h_{max} = (P_{max}/\gamma)$ maximum head of dynamic pressure fluctuation;
P_{max} = maximum dynamic pressure fluctuation;
$h_{min} = (P_{min}/\gamma)$ minimum head of dynamic pressure fluctuation;
P_{min} = minimum dynamic pressure fluctuation;
$h_p = (P_p/\gamma)$ head of dynamic pressure or average pressure fluctuation ;
P_p = average dynamic pressure fluctuation;
r^2 = correlation factor
$\zeta = Fr_0^{0.65} \times tan\alpha$ entrance number
$X_{Pmin} = x_{Pmin}/L_t$ dimensionless location of minimum dynamic pressure fluctuation
x_{Pmin} = location of minimum dynamic pressure fluctuation
$\delta = (h - h_v)/(V^2/2g)$ Cavitation index;
h_v = vapor pressure head;

[DOI: 10.22068/IJCE.13.1.45]

h = absolute pressure head
h_{PM} = maximum dynamic pressure head;
X_{PM} = x/x_{PM} relative location of the maximal measured pressure head;
x_{PM} = location of maximum measured dynamic pressure head
$\eta = sin\theta / (sin\alpha + sin\theta)$ Angle number
$P^* = h_p/h_{PM}$ relative pressure
τ = fitting parameter

References

[1] Vischer DL, Hager WH. Energy dissipators, Balkema, Rotterdam, The Netherlands, 1995.
[2] Vischer DL, Hager WH. Dam hydraulics, John Wiley & Sons, Chichester, UK, 1998.
[3] Khatsuria RM. Hydraulics of spillways and energy dissipators, Dekker, New York, 2005.
[4] Novak P, Moffat AIB, Nalluri C, Narayanan R. Hydraulic structures, Spon, London, 2006.
[5] Balloffe A. Pressures on spillway flip buckets, Journal of the Hydraulics Division, ASCE, 1961, No. 5, Vol. 87, pp. 87–98.
[6] Henderson FM, Tierney DG. Flow at the toe of a spillway, La Houille Blanche, Grenoble, France, 1963, No. 1, Vol. 18, pp. 42-50.
[7] Chen TC, Yu YS. Pressure distribution on spillway flip buckets, Journal of the Hydraulics Division, ASCE, 1965, No. 2, Vol. 91, pp. 51-63.
[8] Lenau CW, Cassidy JJ. Flow through spillway flip bucket, Journal of the Hydraulics Division, ASCE, 1969, No. 5, Vol. 95, pp. 633-648.
[9] Varshney RS, Bajaj ML. Ski-jump buckets on Indian dams, Water and Energy International, 1970, No. 4, Vol. 27, pp. 383-393.
[10] Rajan BH, Shivashankara Rao KN. Design of trajectory buckets, Water and Energy International, 1980, No. 1, Vol. 37, pp. 63-76.
[11] Shivashankara Rao KN. (). "Design of energy dissipators for large capacity spillways." Proc., Brazilian Committee on Large Dams, Rio de Janeiro, Brazil, 1982, Vol. 1, pp. 311-328.
[12] Juon R, Hager WH. Flip bucket without and with deflectors, Journal of Hydraulic Engineering, 2000, No. 11, Vol. 126, pp. 837-845.
[13] Heller V, Hager WH, Minor HE. Ski jump hydraulics, Journal of Hydraulic Engineering, 2005, No. 5, Vol. 131, pp. 347-355.
[14] Steiner R, Heller V, Hager WH, Minor HE. Deflector ski jump hydraulics, Journal of Hydraulic Engineering, 2008, No. 5, Vol. 134, pp. 562-571.
[15] Yamini OA, Kvianpour MR. Experimental study of static and dynamic pressures over simple flip bucket, 5th Symposium on Advances in Science & Technology, Mashhad, Iran, 2011.
[16] Kerman Nejad J, Fathi Moghadam M. Dynamic pressure of flip bucket jets, World Applied Sciences Journal, 2011, No. 9, Vol. 12, pp. 1448-1454.
[17] Margot X, Hoyas S, Gil A, Patouna S. Numerical modelling of cavitation: validation and parametric studies, Engineering Applications of Computational Fluid Mechanics, 2012, No. 1, Vol. 6, pp. 15-24.
[18] Mahmoud H, Kriaa W, Mhiri H, Le Palec G, Bournot P. Numerical analysis of recirculation bubble sizes of turbulent co-flowing jet, Engineering Applications of Computational Fluid Mechanics, 2012, No. 1, Vol. 6, pp. 58-73.
[19] Chau KW, Jiang YW. A three-dimensional pollutant transport model in orthogonal curvilinear and sigma coordinate system for Pearl river estuary, International Journal of Environment and Pollution, 2004, No. 2, Vol. 21, pp. 188-198.
[20] Wu CL, Chau KW. Mathematical model of water quality rehabilitation with rainwater utilization - a case study at Haigang, International Journal of Environment and Pollution, 2006, Nos. 3-4, Vol. 28, pp. 534-545.
[21] Chau KW, Jiang Y. 3D numerical model for Pearl River estuary, Journal of Hydraulic Engineering, ASCE, 2001, No. 1, Vol. 127, pp. 72-82.
[22] Lopardo R. Stilling basin pressure fluctuations. in model–prototype correlations of hydraulic structures, Proceedings of the International Symposium ASCE, Colorado Springs, (ed. P. H. Burgi), American Society of Civil Engineers, New York, 1988, pp. 56-73.
[23] Novak P, Cabelka J. Model in Hydraulic Engineering, Pitman Advanced Publishing Program, London, 1981.
[24] McCuen RH, Leahy RB, Johnson PA. Problems with logarithmic transformations in regression, Journal of Hydraulic Engineering, ASCE, 1990, No. 3, Vol. 116, pp. 414-428.

[DOI: 10.22068/IJCE.13.1.45]